

# Autoencoder-Based Enhancement of Daltonized Images for Color Vision Deficiency (CVD): A Comparative Study with Glass-Based Correction

Taneem Ahmed

*Electrical and Computer Engineering  
North South University  
Dhaka, Bangladesh  
taneem.ahmed@northsouth.edu*

Siddhartha Sankar Saha

*Electrical and Computer Engineering  
North South University  
Dhaka, Bangladesh  
siddhartha.saha@northsouth.edu*

Writhy Tahsin

*Electrical and Computer Engineering  
North South University  
Dhaka, Bangladesh  
writhy.tahsin@northsouth.edu*

Mahbub Morshed Rifat

*Electrical and Computer Engineering  
North South University  
Dhaka, Bangladesh  
mahbub.rifat@northsouth.edu*

Dr. Mohammad Ashrafuzzaman Khan

*Electrical and Computer Engineering  
North South University  
Dhaka, Bangladesh  
mohammad.khan02@northsouth.edu*

**Abstract**—Color vision deficiency is the most common difficulty every human being faces. Currently, medical science lacks a long-term remedy. The subject of this research is to expose artificial intelligence methods as profound studies that aim at material, tangible visualization through images of color blindness in humanity, hence becoming a hope that technology will eventually fill the gap in color perception. The first model is Daltonization, which simulates the perception of color by different kinds of CVD and hence can create image transformations that specifically cater to one's eye problems. Secondly, our proposed CNN-based Autoencoder model, trains on various images taken under normal vision color conditions and daltonized color vision deficiency (CVD) conditions. Therefore, the aim is to create an autoencoder that will convert any image into a better-colored one that is visible to individuals suffering from CVDs. The triumph of this task is determined by how well it performs in terms of two criteria. Quantitative measurements allow for an analysis of the degree to which the latest picture reproduces original images through performance metric like SSIM (Structural Similarity Index Measure), MS-SSIM (Multi Scale SSIM), PSNR (Peak Signal-to-Noise Ratio) and LPIPS (Learned Perceptual Image Patch Similarity). We further validated our approach through comprehensive comparison with traditional glass-based correction methods, demonstrating significant improvements in color distinguishability (22.9% increase in distinct colors against vino) and reduction in color confusion (29% improvement in CCI against enchroma-cx1) while maintaining real-time processing capabilities. User testing and feedback obtained from people suffering from CVD constitute quality appraisals for verifying the acceptability of changes made to their visual perception.

**Index Terms**—Protanopia, Deutanopia, Tritanopia, Daltonization, Deep Learning, CNN, Autoencoder, SSIM, MS-SSIM, PSNR, LPIPS, Glass Effect, Delta E, CCI, Contrast, Color Variance, Distinct Colors

## I. INTRODUCTION

Daltonization is a technique that adjusts image colors to support people with color vision deficiency (CVD), commonly

known as color blindness. It is designed to modify the colors in an image in such a way that people with color vision deficiency can distinguish the differences between colors that are difficult for them to distinguish [12]. Our research aims to demonstrate AI methods, such as deep learning, to make images more tangible to people with color vision deficiency. The goal of employing models like the CNN-based neural network Autoencoder model on Daltonization is to create personalized image representations that cater to their specific visual needs. Our research paves the way for a future where technology bridges the gap in color perception.

**Motivation:** Color vision deficiency (CVD) has been a common worldwide phenomenon in recent years. Color vision deficiency (CVD) has been a common worldwide phenomenon in recent years. Being a genetic disorder, it is increasing day by day. Currently, 300 million people live with color vision problems. All twelve men (8%) and one in two hundred women (0.5%) have CVD. In 1974, John Dalton first described the color blindness problem. He and his brother were also colorblind. They are often confused with green and pink with blue. John Dalton was instructed to examine his eyes perfectly after his death. Later, DNA extraction of his preserved eye tissue revealed that he was deutanope, which means he lacks the middle wave photopigment of the retina. However, in the early 20th century, everyone started to pay attention. [6]

The research aims to improve the people's lives with color vision deficiency, which motivates us. Difficulty in distinguishing color hampers everyone's daily life. It pushes them to depend on others. They require assistance comprehending traffic lights but no information about color blindness. Generally, there exist three classes of color blindness.

- 1) **Red-Green Color Blindness:** This is the most com-

monly seen case where people cannot distinguish reds from greens.

- 2) **Blue-Yellow Color Blindness:** This type comes next after blue-yellow color blindness because it entails an inability to differentiate between blues and yellows.
- 3) **Complete Color Blindness (Achromatopsia):** Few individuals experience total achromatopsia despite its scarcity; hence, they see the world in gray color.

Human color vision is accomplished through cone cells in the retina. A human with typical vision will have three types of cells sensitive to different light wavelengths. The L-cones catch the Long-wavelength (red), M-cones catch the Medium wavelength (green), and S-cones catch the Short-wavelength (blue). Cone-related CVD types:

- 1) **Monochromacy:** This is the worst form of CVD. In this, only a single type of cone is working, or no cone is working at all. The people having monochromacy see a gray world.
- 2) **Dichromacy:** It is more common than the previous one. A person will be having two types of cones. About these, there are several types of dichromacy according to which type of cone is missing:
  - a) **Protanopia:** Missing or malfunctioning L-cones (red).
  - b) **Deutanopia:** Missing or malfunctioning M-cones (green).
  - c) **Tritanopia:** Missing or malfunctioning S-cones (blue).
- 3) **Anomalous Trichromacy:** This is the most common form of CVD; the sensitivity of one of the three normal cones is changed. Following are the types of anomalous trichromacy according to the changed cone:
  - a) **Protanomaly:** L-cone sensitivity is different.
  - b) **Deutanomaly:** M-cone sensitivity is different.
  - c) **Tritanomaly:** S-cone sensitivity is different.

Personal experiences, social impact, design challenges, technology advancements, awareness, educational value, entrepreneurial spirit, and social impact have driven us to choose color vision deficiency. It is a passion to find solutions and make a change due to the challenges faced by individuals with color vision deficiency. The potential for broad social impact and inventive solutions can result in a more inclusive society. Color blindness comes with unique design problems, which may motivate individuals who are into creativity in solving problems. Lessening the effect of CVD and supporting inclusiveness will reduce the stigmatization around it while fostering an all-encompassing society.

However, traditional approaches to CVD assistance have primarily focused on physical solutions such as color-correcting glasses and contact lenses. While these optical methods can provide some enhancement, they suffer from limitations including high cost, limited availability, and inability to adapt to diverse visual environments. More recently, digital solutions have emerged that leverage image processing algorithms to modify content in real-time, offering

potentially more accessible and customizable alternatives. However, comprehensive comparisons between these digital approaches and established physical methods remain scarce in the literature. Our research addresses this gap by conducting a rigorous comparative evaluation between our deep learning-based autoencoder and simulated glass-based correction, providing valuable insights into the relative strengths and limitations of each approach for practical CVD assistance.

**Contributions:** The overarching aim of this project was to contribute to the enhancement of color vision deficiency (CVD) research by addressing the following specific goals.

- 1) We gathered diverse image datasets from sources like Kaggle, Hugging Face, and websites such as Unsplash and Pixels. Our project utilized a customized dataset that mixed all the collected images.
- 2) We employed various generative models, including CGAN, Stable Diffusion, VAE, and AE, to differentiate the quality of daltonized images.
- 3) We comprehensively evaluated our model's performance using multiple metrics: MS-SSIM loss as the primary training objective, alongside PSNR for reconstruction quality, LPIPS for perceptual similarity, and SSIM for structural fidelity while maintaining real-time inference speeds over 300 FPS across all colorblind types.
- 4) To enhance the model's interpretability and transparency, we applied generative, feature-extraction model which helped to illuminate the models' decision-making processes, enabling us and other professionals to better comprehend and trust the outcomes.
- 5) We conducted a comprehensive comparative evaluation against traditional glass-based correction methods, demonstrating our autoencoder's superiority with significant improvements in some CVD specific measures while maintaining real-time processing capability.

**Organization:** Section II briefly discusses notable existing work related to color vision deficiency problem. Section III highlights how we have collected our data and made our synthetic dataset to train our deep learning model. Section IV elaborates our rationality to design our model architecture with specific blocks and their parameters to solve this problem. Section V describes our research methods, techniques, or approaches to solve the problem. Section VI represents the research findings or results and discussion regarding solving the problem. Finally, Section VII shows a comparative evaluation with glass-based correction methods to solidify our approach.

## II. RELATED WORK

A team of researchers led by Xuming Shen at Hangzhou Dianzi University unveiled a noble content-dependent Daltonization algorithm to help people with color vision deficiencies better sense color through lightness and chroma information. The developed algorithm was focused on previous challenges with the need to increase contrast and,

at the same time, ensure consistency in natural colors. The algorithm provided better color consistency characteristics for those CVDs than other methods, which is of utmost significance regarding color perception. According to the study, this new algorithm for correcting color perception in CVD users is subject to possible errors or limitations, such as color shifts due to luminance modifications and reliance on clustering mechanisms for image processing. This generates artifacts in the image, so it is not recommended for videos. Real-time video processing using image processing techniques will be a part of our future study. We will conduct experiments on enhancing image segmentation and at the perceptual learning level for CVD users in the future. [14]

In work by Christos-Nikolaos Anagnostopoulos, George Tsekouras, Ioannis Anagnostopoulos, and Christos Kalloniatis, a method to maximize digital image viewing experience for protanopic individuals has been created. It mixes up red and greens in some forms of color-blindness. The process converts the standard RGB color space into a dichromatic version, imitating red-blind color perception (protanopia). The RGB similarity-checking module guarantees that the adaptation parameters are intelligently selected, not by trial and error. The RGB similarity-checking module determines the outer lateral tapering of each color set on correcting the error matrix to ensure that the original image and the daltonized image will not match if a color is within the tolerance level. For example, a color tolerance of 21 would designate that a range of colors in C ( $100\pm10$ ,  $150\pm10$ ,  $130\pm10$ ) are sufficiently close to C2 (100, 150, 130). The algorithm requires 2.1 seconds per iteration on a Pentium IV 3.2 GHz processor, making it impossible to use for real-life video image processing. It is because the algorithm can be made applicable to other color vision weaknesses, but it is currently tailored exclusively to protanopia. Future work needs to center on optimizing the existing algorithms and then on implementing efficiency and extending the use for other color vision deficiencies. [1]

Jinmi Lee and Wellington dos Santos (2017) created DaltonTest, an adaptive fuzzy simulation tool designed to improve color perception for users with color vision deficiencies. The tool uses the Ishihara test for color blindness and then applies adaptive filtering to digital images. The two methods proposed are Method A, which is a correction of absolute color blindness with the use of fuzzy rules, and Method B, which is a correction using linear transformations for adaptive correction based on fuzzy degrees of protanomaly and deutanomaly. Ordinary and color-blind people tested the A tool on both. The first phase of testing showed that correcting in the RGB domain with the help of histogram equalization enhanced image understanding and decreased the original colors' distortions. Non-color-blind users were the only ones. Ten basic images simulated protan and deuteron color blindness at different intensities. Method B, which used histogram equalization, was the most effective, and it

got 47.3% of positive answers for protan color blindness. The study's limitation is the lack of mathematical techniques for adaptive color blindness compensation and the limited real color blindness cases. Notwithstanding, the encouraging outcomes imply that fuzzy-based methods could help color perception for people with color vision deficiencies. Further research is necessary to make these methods more applicable to other types of color blindness. [7]

Li et al. (2020) introduces an innovative approach to help individuals with color vision deficiency perceive color better. The database includes 5,699 images recolored using an optimization-based and self-adapting rule-based algorithm. The effectiveness of the dataset is tested by training three GAN networks: pix2pix-GAN, Cycle-GAN, and Bicycle-GAN. According to the results, pictures-to-pictures GAN does significantly better regarding both subjective and objective scores over Cycle-GAN, whereas Bicycle-GAN provides much blurrier images. The nice thing about this paper is the optimistic view on the CVD image recolorization capacity of learning methods based on deep learning. However, it highlights limitations such as a limited dataset, a self-adaptive algorithm, and quantitative evaluation methods. Now, we need a more extensive dataset and improved color-matching algorithms. [8]

### III. DATASET

First, we downloaded the dataset of places pictures from Kaggle; afterwards, we used a Daltonization algorithm [5] on the whole dataset to create enormous variations and types of data to train and validate our model.

#### A. Real Dataset

For this research, we have used the Kaggle places pictures dataset(<https://www.kaggle.com/datasets/mittalshubham/images256>). is a subset of the MIT CSAIL Places dataset, containing 10% of the original data with images resized to 256x256 pixels. It includes a total of 205 classes representing diverse scene categories. This dataset is commonly used for computer vision research, providing a manageable portion of the large original dataset for easier experimentation and model training while preserving the diversity of classes.

#### B. Synthetic Dataset

We have used the Daltonization algorithm in the Kaggle data set to make the three different types (protanopia, deutanopia and tritanopia) daltonized versions. Along with the 4319 original images, our custom dataset contains  $35604 + 35604*3 = 1,42,416$  images.

We defined a dataset class in PyTorch, which helped us to easily train a model for color-blindness correction or simulation. We loaded pairs of images from a specified directory, where each pair contains the original image and its modified daltonized version that simulates one of the possible types of color blindness. We perform transformations such as resizing, conversion to tensors, and normalization to prepare the images for the model. The data set can now be easily used in training

loops to feed the model with the original and color-blind image pairs to learn the transformations needed to correct or simulate color vision deficiencies.

Applying all preprocessing steps to the collected data: First, we had ensured that the input image is in torch.float32, the standard type for PyTorch tensors. Then, the pixel values were normalized to the range between 0 and 1, followed by rescaling by 0.5. Further, our transformation pipeline resized the image to 256x256 pixels, transformed it into a PyTorch tensor, and performed normalization again by subtracting the mean–0.5 for each color channel and dividing by the standard deviation–0.5. Our standardized format is important for effective learning in most image-based deep-learning tasks.

Lastly We divided the dataset into training, validation, and testing sets in the proportion of 8 : 1 : 1 (approximately). The modified autoencoder model, categorized by types, was trained on the training set, validated using the validation set, and its performance was finally evaluated on the test set.

TABLE I  
DATASET (IMAGES)

Set	Original	Protanope	Deutanope	Tritanope
Training Set	29670	29670	29670	29670
Validation Set	2967	2967	2967	2967
Test Set	2967	2967	2967	2967

#### IV. MODEL ARCHITECTURE

Enhancing the daltonized images using deep learning, we have looked at Stable Diffusion models, GANs, Conditional GANs, and VAE. We selected the most suitable architecture based on the visualization and SSIM performance curve for the final research. This chosen backbone architecture was based on a CNN-based Autoencoder with skip connections that would form the backbone for our daltonized generating model, ensuring accurate performance.

In our proposed *Autoencoder-based Enhancement of Daltonized Images for Color Vision Deficiency (CVD): A Comparative Study with Glass-Based Correction* architecture, we introduced two blocks as the building blocks of our model: *ConvolutionalBlock*, & *DeconvolutionalBlock* which also have skip connections. These blocks are responsible for capturing and propagating important features through the network, facilitating the enhancement of daltonized results.

**Convolutional Block:** The ConvolutionalBlock is designed to handle down-sampling operations in the network. It begins with a 2D convolutional layer (nn.Conv2d) that takes an input with 3 color channels (typically an RGB image) and applies kernels of size 3x3, with a stride of 2 and padding of 1. The stride of 2 reduces the spatial dimensions of the input image by half, while the padding of 1 ensures that the spatial dimensions are preserved at the edges. Batch normalization is applied to stabilize the learning process and improve the efficiency of the network. Additionally, ReLU applies the Rectified Linear Unit activation function, introducing non-linearity to the model and helping it learn complex patterns.

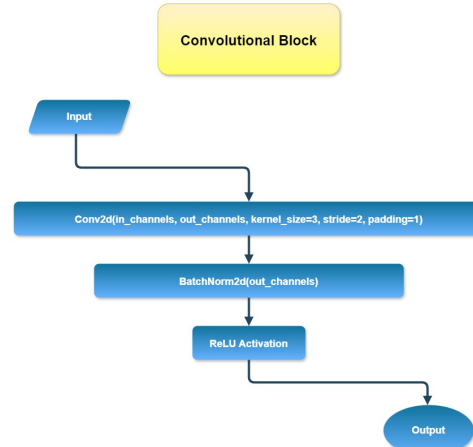


Fig. 1. Convolutional Block

**Deconvolutional Block:** This DeconvolutionalBlock is designed for upsampling in a neural network. This sequential layer, in which each layer performs 2D transposed convolutions (nn.ConvTranspose2d), serves to increase the spatial dimensions of the input feature maps, hence effectively upsampling them. The kernel size is 4x4, the stride is 2, and the padding is 1; this configuration doubles the spatial dimensions with each ConvTranspose2d layer. Each block is followed by the use of batch normalization for normalizing the output to stabilize training and ReLU for non-linearity, except that the last block uses the Sigmoid Function, mapping the output values in the range [0, 1] suitable for generating final image outputs.

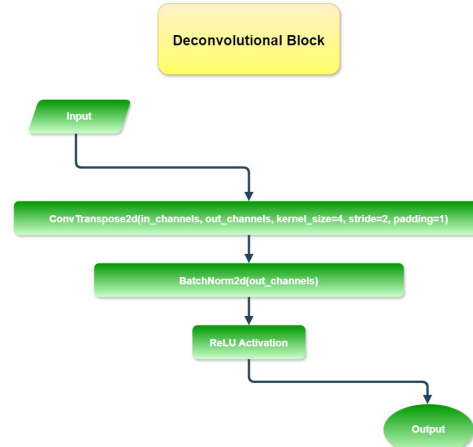


Fig. 2. Deconvolutional Block

**Autoencoder Architecture:** In our proposed Autoencoder architecture, we start out with an encoding journey where we progressively down-sample the input image through convolutional layers. The meaningful features of the input image are extracted by the encoder through a series of convolutional and activation layers. These layers progressively reduce their

spatial dimensions with an increasing number of channels, thus enabling the network to capture higher levels of image representation. The process finally distills the image into a compact latent representation.

While the encoder portion has the job of encoding the image into the latent representation, the decoder component takes the latent representation to rebuild the image. It basically is a mirror of the encoder structure in reverse, focusing on deconvolutional layers for upsampling the features to regenerate the image with its corresponding color information.

In the process, the autoencoder is trained to minimize the reconstruction error between the original input image and the output image generated by the decoder. By this process, the autoencoder learns the important features that are to be utilized in the proper reconstruction of images.

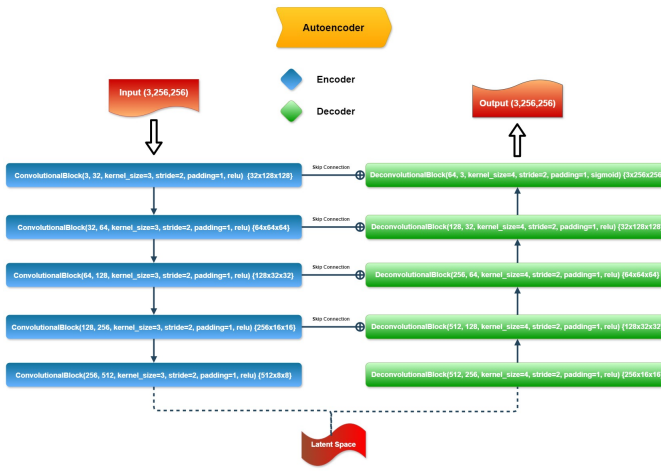


Fig. 3. Autoencoder

## V. EXPERIMENTS

**Experimental Setup:** The experiment aims at developing an autoencoder model for color vision deficiency correction. We did this by training a dataset containing images that represented various scenes as seen through the eyes of people with various types of color blindness: protanopia, deutanopia, and tritanopia, on a deep convolutional neural network. Our preprocessing consists of resizing images and applying normalization to enhance the model's generalization ability. The architecture of the autoencoder includes skip connections that improve the reconstruction quality, learning a compact representation of the input images to generate the color-corrected versions. The model is evaluated using the Structural Similarity Index Measure (SSIM), Peak Signal-to-Noise Ratio (PSNR), and Learned Perceptual Image Patch Similarity (LPIPS)—comprehensive perceptual quality assessment metrics that measure structural fidelity, signal clarity, and perceptual similarity, respectively. The mathematical definitions of the evaluation metrics are:

### A. Multi-Scale Structural Similarity Index Loss

The primary training objective is defined as:

$$\mathcal{L}_{\text{MS-SSIM}} = 1 - \text{MS-SSIM}(I_{\text{output}}, I_{\text{target}}) \quad (1)$$

where MS-SSIM is computed across multiple scales:

$$\text{MS-SSIM}(x, y) = [l_M(x, y)]^{\alpha_M} \cdot \prod_{j=1}^M [c_j(x, y)]^{\beta_j} [s_j(x, y)]^{\gamma_j} \quad (2)$$

where:

- $l_M(x, y) = \frac{2\mu_x\mu_y + C_1}{\mu_x^2 + \mu_y^2 + C_1}$  is the luminance comparison at scale M
- $c_j(x, y) = \frac{2\sigma_x\sigma_y + C_2}{\sigma_x^2 + \sigma_y^2 + C_2}$  is the contrast comparison at scale j
- $s_j(x, y) = \frac{\sigma_{xy} + C_3}{\sigma_x\sigma_y + C_3}$  is the structure comparison at scale j
- $\mu_x, \mu_y$  are local means of images x and y
- $\sigma_x^2, \sigma_y^2$  are local variances of images x and y
- $\sigma_{xy}$  is the local covariance between x and y
- $\alpha_M, \beta_j, \gamma_j$  are weights for each component
- $C_1, C_2, C_3$  are small constants for numerical stability
- $I_{\text{output}}, I_{\text{target}} \in [-1, 1]$  are the model output and target images normalized to the  $[-1, 1]$  range, and MS-SSIM is computed with a dynamic range of 2.0.

### B. Peak Signal-to-Noise Ratio

$$\text{PSNR} = 10 \cdot \log_{10} \left( \frac{1}{\text{MSE}_{\text{scaled}}} \right) \quad (3)$$

where the mean squared error is calculated on images scaled to  $[0, 1]$  range:

$$\text{MSE}_{\text{scaled}} = \frac{1}{N} \sum_{i=1}^N \left( \frac{I_{\text{target}}(i) + 1}{2} - \frac{I_{\text{output}}(i) + 1}{2} \right)^2 \quad (4)$$

and N is the total number of pixels, with maximum possible pixel value of 1.0.

### C. Learned Perceptual Image Patch Similarity

$$\text{LPIPS} = \frac{1}{L} \sum_{l=1}^L \frac{1}{H_l W_l C_l} \sum_{h,w,c} \|w_l \cdot \Delta\phi_{hwc}^l\|^2 \quad (5)$$

where:

- $\Delta\phi_{hwc}^l = \phi_l(I_{\text{output}})_{hwc} - \phi_l(I_{\text{target}})_{hwc}$
- $\phi_l(\cdot)$  represents features extracted from layer l of a pre-trained AlexNet
- $H_l, W_l, C_l$  are the height, width, and channel dimensions at layer l
- $w_l$  are learned weights for layer l
- $I_{\text{output}}, I_{\text{target}} \in [-1, 1]$  are the input images

#### D. Structural Similarity Index

$$\text{SSIM}(I_{\text{output}}, I_{\text{target}}) = \frac{(2\mu_x\mu_y + C_1)(2\sigma_{xy} + C_2)}{(\mu_x^2 + \mu_y^2 + C_1)(\sigma_x^2 + \sigma_y^2 + C_2)} \quad (6)$$

where:

- $\mu_x, \mu_y$  are the local means of  $I_{\text{output}}$  and  $I_{\text{target}}$
- $\sigma_x^2, \sigma_y^2$  are the local variances
- $\sigma_{xy}$  is the local covariance
- $C_1 = (0.01 \times 2)^2, C_2 = (0.03 \times 2)^2$  for images in  $[-1, 1]$  range

#### E. Implementation Details

All metrics were computed on GPU using:

- **MS-SSIM:** Primary loss function with data range 2.0
- **PSNR:** Calculated after scaling images to  $[0, 1]$  range
- **LPIPS:** AlexNet backbone with images in  $[-1, 1]$  range
- **SSIM:** Computed with data range 2.0 for  $[-1, 1]$  normalized images
- **Training:** Automatic Mixed Precision (AMP) with early stopping (patience=5)

In the training process, we run over the number of epochs to 50. We set the batch size to 16. We load images from our dataset in batches in each epoch and feed them into the autoencoder. After a forward pass, it generates the images reconstructed; then, we calculate the loss with the corresponding colorblind images.

The weights of the model in training were optimized using the Adam optimizer. We set the learning rate to 0.0001, which determines the step size for updating the model's parameters during optimization. Essentially, optimizer is used to tune the parameters of the model by considering the gradient in the loss function in an incremental manner to improve the color feature detection capability of the model.

**Evaluation:** As the loss function, we used MS-SSIM (Multi-Scale Structural Similarity), which guides the training of neural networks toward the synthesis of images that are perceptually similar to target images. The MS-SSIM measures the dissimilarity (1 - MS-SSIM) of the generated image from the target image across multiple scales, hence encouraging the optimization of the network in the generation of local details and structure of the image as a whole, which results in outputs closer to human perception.

The Adam optimizer tuned the model parameters based on this calculated loss. To comprehensively evaluate model performance beyond the primary loss, we tracked several key metrics at each training and validation epoch. These included the primary MS-SSIM Loss, Peak Signal-to-Noise Ratio (PSNR) to measure reconstruction fidelity at a pixel level, LPIPS (Learned Perceptual Image Patch Similarity) to assess perceptual quality using a deep learning model, and SSIM (Structural Similarity Index Measure) for an additional measure of structural preservation.

This multi-faceted evaluation provided a holistic view of the model's performance, balancing pixel-level accuracy with perceptual quality. Images in both the original and colorblind formats, along with the reconstructed images for each kind of colorblindness, were visualized throughout both training and validation. By the end of this process, we had an autoencoder model trained to restore color vision, rigorously evaluated across a suite of complementary metrics.

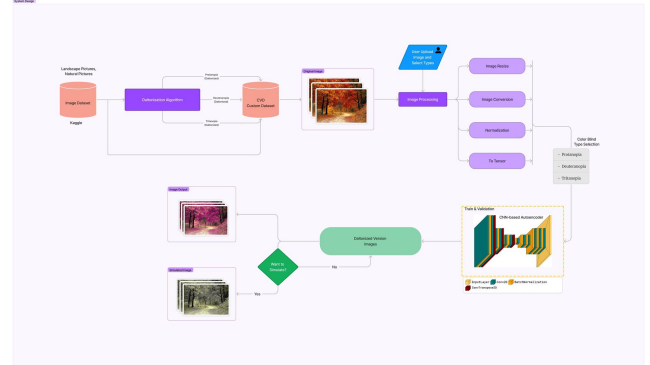


Fig. 4. System Design

## VI. RESULTS

The performance of our daltonized CNN-based autoencoder models was comprehensively evaluated across three colorblindness types (protanopia, deutanopia, and tritanopia) using multiple perceptual and quantitative metrics: 1-MS-SSIM Loss, Structural Similarity Index Measure (SSIM), Peak Signal-to-Noise Ratio (PSNR), and Learned Perceptual Image Patch Similarity (LPIPS). The models demonstrated consistent learning across all types with early stopping implemented to prevent overfitting.

TABLE II  
COMPARATIVE PERFORMANCE ANALYSIS OF DALTONIZATION MODELS

Metric	Protanopia	Deutanopia	Tritanopia
MS-SSIM Loss	0.0113	<b>0.0109</b>	0.0157
SSIM	0.9125	<b>0.9174</b>	0.9041
PSNR (dB)	28.39	<b>29.51</b>	27.98
LPIPS	0.0478	<b>0.0382</b>	0.0392
Inference Speed (FPS)	303.4	<b>304.2</b>	287.2

**Overall Performance Analysis:** The models achieved excellent performance across all colorblind types, with deutanopia showing the best overall results (lowest MS-SSIM loss of 0.0109, highest SSIM of 0.9174, and best PSNR of 29.51 dB). All models demonstrated strong generalization capabilities on the test set, with SSIM scores consistently above 0.90, indicating high structural similarity between generated and target images. The LPIPS scores below 0.05 across all

types confirm excellent perceptual quality in the reconstructed images.



Fig. 5. Comprehensive Training Metrics for Protanopia

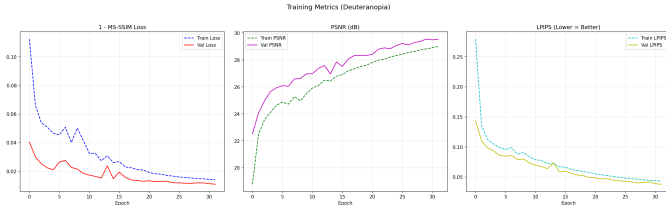


Fig. 6. Comprehensive Training Metrics for Deuteranopia



Fig. 7. Comprehensive Training Metrics for Tritanopia

**Training Dynamics Analysis:** The learning curves for protanopia (Figure 5) demonstrate rapid improvement in the initial epochs, with MS-SSIM loss decreasing from 0.1130 to 0.0113, PSNR increasing from 19.19 dB to 28.39 dB, and LPIPS improving from 0.2612 to 0.0478. Similar trends were observed for deuteranopia and tritanopia, with all models showing consistent convergence behavior. The parallel improvement across all metrics indicates balanced learning that optimizes both pixel-level accuracy (PSNR) and perceptual quality (LPIPS, MS-SSIM).

**Convergence and Early Stopping:** The models employed early stopping with a patience of 5 epochs, with protanopia stopping at epoch 26, deuteranopia at epoch 32, and tritanopia at epoch 28. This indicates efficient training without overfitting, as validation metrics continued to improve throughout the training process. The consistent gap between training and validation metrics across all types suggests appropriate model capacity and regularization.

**Inference Performance:** The models demonstrated real-time capability with inference speeds exceeding 280 FPS across all types (protanopia: 303.4 FPS, deuteranopia: 304.2 FPS,

tritanopia: 287.2 FPS), making them suitable for practical applications requiring rapid image processing.

Overall, the multi-metric evaluation confirms that the autoencoder models successfully learned to reconstruct color-corrected images with high perceptual quality and structural fidelity across all colorblindness types, with deuteranopia showing slightly superior performance compared to protanopia and tritanopia.

## Daltonized Outcomes:

### A. Protanopia (Missing or malfunctioning L-cones: Red)

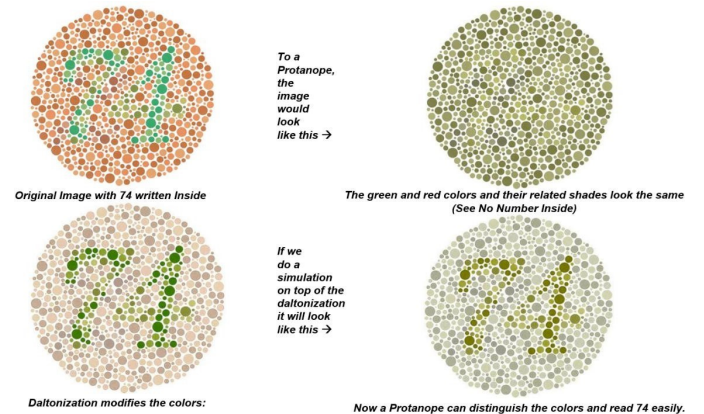


Fig. 8. Protanopia Result (Ishihara)

### B. Deuteranopia (Missing or malfunctioning M-cones: Green)

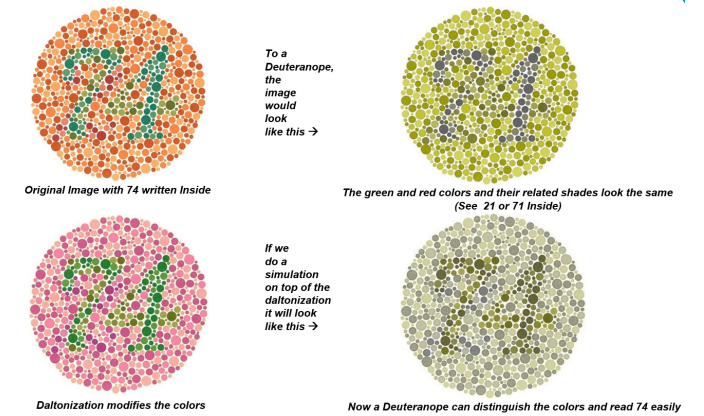


Fig. 9. Deuteranopia Result (Ishihara)

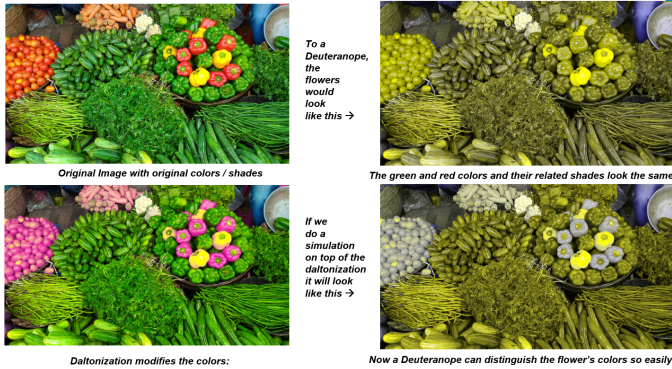


Fig. 10. Deutanopia Result

### C. Tritanopia (Missing or malfunctioning M-cones: Blue)

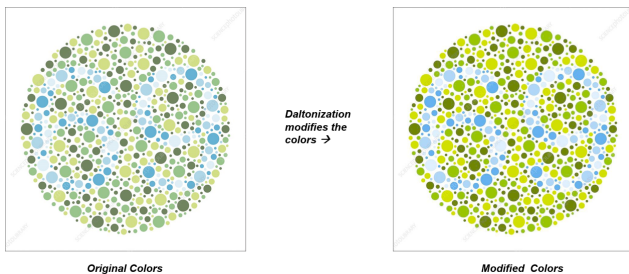


Fig. 11. Tritanopia Result (Ishihara)

**Analysing Images with Color Shades:** If we look at results with various shades of color, it is easy to realize how hard it is to tell the difference in colors for a person with color deficiency. The shades often mix together. The human eye can detect approximately 10 million shades of color. So, our generated results suggest that an enhanced range of shades according to the perception of the color-deficient observer will allow them to pick out colors more easily.

- **First Observation:** If we could see the picture, there are many shades of colors that the human eye can perceive in the flower. Some of its main shades are shown in the suggested color palette. There are also many other shades of these colors.



Fig. 12. Original Image

- **Second Observation:** Suppose we simulate the image to show how a person with deuteranopia, that is, red/green color blindness, can see the colors and shades of the flowers. Then we will see that for them, the colors and shades are quite similar, overlapping, and therefore indistinguishable.



Fig. 13. Deutanopia Simulation

- **Third Observation:** The Daltonization algorithm works wonders in balancing color while holding the same content meaning. It recolors most of the indistinguishable colors into a form that allows color-deficient people to see most colors within their color palettes.



Fig. 14. Deutanopia Daltonization

- **Final Observation:** Finally, running the simulation of the Daltonized version, we observe that more colors are seen within the palettes. The missing cones in their retinas do not allow them to visualize the colors, and they need medical treatment. However, they can observe more colors and will discern colors, objects, and letters better than usual.



Fig. 15. Deuteranopia Daltonized & Simulation

### CNN based Autoencoder Outcomes:

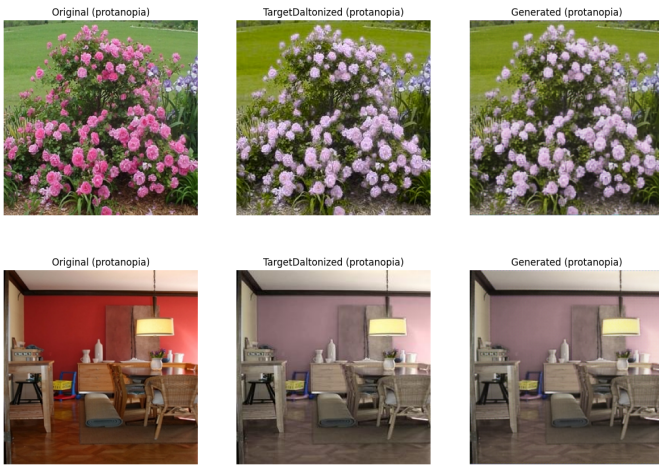


Fig. 16. Original , Daltonized & Autoencoder (CNN) Versions: **Protanopia**



Fig. 17. Original , Daltonized & Autoencoder (CNN) Versions: **Deuteranopia**



Fig. 18. Original , Daltonized & Autoencoder (CNN) Versions: **Tritanopia**

Our research has focused on the potential of autoencoders, the types of deep learning models, in enhancing the quality of images that are subjected to color blindness. The integration of skip connections enabled our model to capture and reconstruct the minute details in the images; this is evidenced by the achievement of high SSIM scores. The plots from the model training process showed a rapid drop in 1-MSSIM loss, indicating that our model was able to quickly grasp the inherent patterns and structures of the input data.

Although our results are promising, there is still room for improvement. Experimentation with other loss functions or architectural changes may further improve the performance of the model.

## VII. COMPARATIVE EVALUATION WITH GLASS-BASED CORRECTION METHODS

### A. Experimental Setup for Comparative Analysis:

To validate the effectiveness of our proposed autoencoder approach, we conducted a comprehensive comparative evaluation against traditional glass-based color correction methods. We implemented a spectral simulation of commercial color-correcting glasses (Vino, Enchroma-CX1) using transmittance data and compared its performance with our daltonized autoencoder across three CVD types: protanopia, deuteranopia, and tritanopia.

### B. Dataset:

We used 100 test images from our dataset, ensuring diverse color compositions and scene types for robust evaluation.

### C. Comparative Methodology:

The glass effect was simulated using spectral transmittance data from commercial CVD-correcting glasses, applying color transformation matrices in the LMS color space to mimic real-world glass performance. Our autoencoder models were evaluated using the same test set with identical pre-processing pipelines to ensure fair comparison. Both methods were

assessed by simulating how a colorblind individual would perceive the corrected images, providing a realistic evaluation of practical utility.

#### D. Glass Effect Spectral Simulation:

The glass effect simulation transforms input images through spectral transmittance data of color-correcting glasses, employing physiological color space transformations to model human visual perception under CVD conditions. The mathematical formulations of glass effect simulation are:

- 1) **Spectral to XYZ Conversion:** The glasses transmittance is converted to CIE XYZ tristimulus values:

$$\mathbf{XYZ}_{\text{glasses}} = \int_{\lambda} T(\lambda) \cdot S_{\text{D65}}(\lambda) \cdot \text{CMFS}_{\text{CIE 1931 } 2^\circ}(\lambda) d\lambda \quad (7)$$

$$\mathbf{XYZ}_{\text{glasses,norm}} = \frac{\mathbf{XYZ}_{\text{glasses}}}{Y_{\text{glasses}}} \quad (8)$$

- 2) **Color Space Transformation Matrices:** The Hunt-Pointer-Estevez transformation matrices:

$$\mathbf{M}_{\text{XYZ} \rightarrow \text{LMS}} = \begin{bmatrix} 0.4002 & 0.7076 & -0.0808 \\ -0.2263 & 1.1653 & 0.0457 \\ 0.0 & 0.0 & 0.9182 \end{bmatrix}, \quad \mathbf{M}_{\text{LMS} \rightarrow \text{XYZ}} = \mathbf{M}_{\text{XYZ} \rightarrow \text{LMS}}^{-1} \quad (9)$$

- 3) **Image Processing Pipeline:**

$$\mathbf{XYZ} = \mathbf{RGB} \cdot \mathbf{M}_{\text{RGB} \rightarrow \text{XYZ}}^{\text{sRGB}} \quad (10)$$

$$\mathbf{LMS} = \mathbf{XYZ} \cdot \mathbf{M}_{\text{XYZ} \rightarrow \text{LMS}}^T \quad (11)$$

$$\mathbf{LMS}_{\text{filtered}} = \mathbf{LMS} \odot [L_{\text{ratio}}, M_{\text{ratio}}, S_{\text{ratio}}] \quad (12)$$

$$\mathbf{XYZ}_{\text{filtered}} = \mathbf{LMS}_{\text{filtered}} \cdot \mathbf{M}_{\text{LMS} \rightarrow \text{XYZ}}^T \quad (13)$$

$$\mathbf{RGB}_{\text{filtered}} = \mathbf{XYZ}_{\text{filtered}} \cdot \mathbf{M}_{\text{XYZ} \rightarrow \text{RGB}}^{\text{sRGB}} \quad (14)$$

where  $[L_{\text{ratio}}, M_{\text{ratio}}, S_{\text{ratio}}] = \mathbf{XYZ}_{\text{glasses,norm}}$

- 4) **Normalization and Clipping:**

$$\mathbf{RGB}_{\text{final}} = \text{clip}\left(\frac{\mathbf{RGB}_{\text{filtered}}}{\max(\mathbf{RGB}_{\text{filtered}}, \epsilon)}, 0, 1\right) \quad (15)$$

with  $\epsilon = 10^{-10}$  for numerical stability.

#### E. Algorithm Implementation

The glass effect simulation follows this computational pipeline:

- 1) Load and normalize input RGB image to  $[0, 1]$  range
- 2) Compute normalized glasses XYZ tristimulus values using D65 illuminant and CIE 1931  $2^\circ$  observer
- 3) Transform image from RGB to XYZ color space using sRGB transformation matrix
- 4) Convert XYZ to LMS cone response space using Hunt-Pointer-Estevez transformation
- 5) Apply glasses filter by scaling LMS responses with normalized XYZ ratios
- 6) Transform filtered LMS back to XYZ color space
- 7) Convert filtered XYZ to RGB using inverse sRGB transformation
- 8) Normalize and clip final RGB values to  $[0, 1]$  range

#### F. Error Handling

The implementation includes robust error handling:

- Invalid images return neutral gray ( $100 \times 100 \times 3$  zeros)
- Division by zero protection with  $\epsilon = 10^{-10}$
- Exception fallback to neutral image or original image float array

#### G. Glasses Data Loading

Spectral transmittance data [11] is loaded from CSV format:

$$T(\lambda) = \text{SpectralDistribution}(\text{values}, \text{wavelengths}) \quad (16)$$

where the dataset contains wavelength (nm) and transmittance pairs.

#### H. Evaluation Metrics:

Beyond traditional metrics, we introduced CVD-specific measures:

- 1) **Delta E (CIEDE2000 Color Difference):** The color difference between reference image  $I_{\text{ref}}$  and test image  $I_{\text{test}}$  is computed as:

$$\Delta E_{00} = \frac{1}{N} \sum_{i=1}^N \Delta E_{\text{CIE2000}}(\mathbf{Lab}_{\text{ref}}(i), \mathbf{Lab}_{\text{test}}(i)) \quad (17)$$

where:

- $\mathbf{Lab}_{\text{ref}} = \text{rgb2lab}(I_{\text{ref}})$
- $\mathbf{Lab}_{\text{test}} = \text{rgb2lab}(I_{\text{test}})$
- $N =$  total number of pixels
- $\Delta E_{\text{CIE2000}}$  implements the complete CIEDE2000 standard from the colour-science library

- 2) **Color Confusion Index (CCI):** The CCI measures color confusion along CVD-specific confusion lines:

$$\text{CCI} = \text{Var}(\mathbf{P} \cdot \mathbf{v}_{\text{cvd}}) \quad (18)$$

with the LMS transformation:

$$\mathbf{P} = \mathbf{RGB} \times \mathbf{M}_{\text{RGB} \rightarrow \text{LMS}}^T \quad (19)$$

where the Hunt-Pointer-Estevez transformation matrix is:

$$\mathbf{M}_{\text{RGB} \rightarrow \text{LMS}} = \begin{bmatrix} 0.4002 & 0.7076 & -0.0808 \\ -0.2263 & 1.1653 & 0.0457 \\ 0.0 & 0.0 & 0.9182 \end{bmatrix} \quad (20)$$

and confusion vectors for different CVD types are:

$$\mathbf{v}_{\text{cvd}} = \begin{cases} [0.0, 2.02344, -2.52581] & \text{for protanopia} \\ [0.0, 0.494207, 0.0] & \text{for deuteranopia} \\ [1.0, 0.0, 0.0] & \text{for tritanopia} \end{cases} \quad (21)$$

3) **Michelson Contrast:**

$$\text{Contrast}(I) = \frac{I_{\max} - I_{\min}}{I_{\max} + I_{\min}} \quad (22)$$

4) **Color Variance:** CVD-optimized color variance uses weighted combination of Lab space variances:

$$\text{ColorVariance} = w_p \cdot \text{Var}(A_p) + w_s \cdot \text{Var}(A_s) \quad (23)$$

where for different CVD types:

- **Protanopia/Deuteranopia:**

$$\begin{aligned} A_p &= b^* \quad (\text{blue-yellow axis, Lab channel 2}) \\ A_s &= L^* \quad (\text{lightness axis, Lab channel 0}) \\ w_p &= 0.7, \quad w_s = 0.3 \end{aligned}$$

- **Tritanopia:**

$$\begin{aligned} A_p &= a^* \quad (\text{red-green axis, Lab channel 1}) \\ A_s &= L^* \quad (\text{lightness axis, Lab channel 0}) \\ w_p &= 0.7, \quad w_s = 0.3 \end{aligned}$$

5) **Distinct Colors:** Let DBSCAN<sub>params</sub> denote DBSCAN clustering with  $\epsilon = 0.3$  and  $\text{min\_samples} = 3$ . Then number of perceptually distinct color clusters using weighted Lab space:

$$\text{DistinctColors} = |\{C \in \text{DBSCAN}_{\text{params}}(\mathbf{L}_{\text{weighted}}) \mid C \neq -1\}| \quad (24)$$

with CVD-optimized weighting:

- **Protanopia/Deuteranopia:**

$$\mathbf{L}_{\text{weighted}} = [1.2 \times L^*, a^*, 1.5 \times b^*] \quad (25)$$

- **Tritanopia:**

$$\mathbf{L}_{\text{weighted}} = [1.2 \times L^*, 1.5 \times a^*, b^*] \quad (26)$$

6) **CVD Effectiveness Score:** Overall performance score for CVD assistance:

$$S_{\text{total}} = \sum_{m \in M} w_m \cdot f_m(I_{\text{ae}}, I_{\text{glass}}) \quad (27)$$

with metric weights:

$$\begin{aligned} w_{\text{ColorVariance}} &= 0.25 \quad \text{or} \quad 0.30 \\ w_{\text{DistinctColors}} &= 0.45 \quad \text{or} \quad 0.30 \\ w_{\text{Contrast}} &= 0.15 \quad \text{or} \quad 0.20 \\ w_{\text{SSIM}} &= 0.10 \quad \text{or} \quad 0.15 \\ w_{\Delta E} &= 0.05 \end{aligned}$$

and scoring functions:

$$f_m(I_{\text{ae}}, I_{\text{glass}}) = \begin{cases} \frac{m(I_{\text{ae}})}{\max(m(I_{\text{ae}}), m(I_{\text{glass}}), \epsilon)} & \text{for } m \in H \\ \frac{m(I_{\text{glass}})}{m(I_{\text{ae}}) + m(I_{\text{glass}})} & \text{for } m = \Delta E \end{cases} \quad (28)$$

where:

- $H = \{\text{ColorVariance}, \text{DistinctColors}, \text{Contrast}, \text{SSIM}\}$  (higher-better metrics)
- $\epsilon = 10^{-10}$  (numerical stability constant)

7) **Implementation Details:**

- All images are normalized to  $[0, 1]$  range
- Invalid images (uniform, zeros, or containing NaN/Inf) are filtered
- Safe division with  $\epsilon = 10^{-10}$  prevents numerical instability
- For small images ( $< 8 \times 8$  pixels), simplified metrics are used

*I. Results and Discussion: AE vs GE*

Our autoencoder demonstrated consistent superiority across all evaluated metrics, with particularly notable improvements in color distinguishability metrics most relevant for CVD assistance.

TABLE III  
OVERALL COMPARATIVE PERFORMANCE: AUTOENCODER VS. VINO  
GLASS EFFECT

Metric	Autoencoder	Vino Glass Effect	Improvement
Delta E	<b>7.340</b>	10.956	+33.0%
Color Confusion Index (CCI)	<b>0.028</b>	0.032	+12.7%
Structural Similarity (SSIM)	<b>0.884</b>	0.860	+2.7%
Contrast	<b>0.996</b>	0.970	+2.7%
Color Variance	<b>216.826</b>	200.025	+8.4%
Distinct Colors	<b>5.817</b>	4.733	+22.9%
CVD Effectiveness Score	<b>0.929</b>	0.838	+10.9%

TABLE IV  
OVERALL COMPARATIVE PERFORMANCE: AUTOENCODER VS.  
ENCHROMA-CX1 GLASS EFFECT

Metric	Autoencoder	Enchroma Glass Effect	Improvement
Delta E	<b>7.340</b>	7.781	+5.7%
Color Confusion Index (CCI)	<b>0.028</b>	0.039	+29.0%
Structural Similarity (SSIM)	<b>0.884</b>	0.910	-2.9%
Contrast	<b>0.996</b>	0.968	+2.9%
Color Variance	<b>216.826</b>	277.448	-21.8%
Distinct Colors	<b>5.767</b>	5.003	+15.3%
CVD Effectiveness Score	<b>0.866</b>	0.851	+1.8%

*Note: Lower values of Delta E and Color Confusion Index (CCI) indicate better color accuracy and reduced confusion, whereas higher values of all other metrics denote improved visual and perceptual quality.*

**Color Distinguishability:** The autoencoder achieved significant improvements in color separation capabilities. Against Vino Glass Effect, it demonstrated 22.9% more distinct colors and 8.4% higher color variance, while against Enchroma-CX1 it maintained 15.3% more distinct colors despite lower color variance. This translates to more distinguishable color boundaries in real-world scenarios like reading charts, maps, and interface elements.

**Color Accuracy:** Our method showed substantial improvements in color accuracy metrics. Compared to Vino Glass Effect, the autoencoder achieved 33% improvement in Delta E and 12.7% reduction in color confusion. Against Enchroma-CX1, it maintained 5.7% better Delta E and 29% lower color confusion index, providing more accurate color perception while maintaining natural image appearance.

TABLE V  
CVD-TYPE SPECIFIC PERFORMANCE: AUTOENCODER VS. VINO GLASS EFFECT

Metric	Protanopia		Deuteranopia		Tritanopia	
	AE	Vino	AE	Vino	AE	Vino
Delta E	<b>6.959</b>	10.555	<b>5.308</b>	7.501	<b>9.753</b>	14.811
CCI	<b>0.025</b>	0.044	<b>0.011</b>	0.009	<b>0.047</b>	0.042
SSIM	<b>0.866</b>	0.875	<b>0.908</b>	0.889	<b>0.878</b>	0.817
Contrast	<b>0.998</b>	0.971	<b>0.995</b>	0.969	<b>0.995</b>	0.971
Color Variance	<b>215.059</b>	210.561	<b>218.611</b>	207.335	<b>216.809</b>	182.179
Distinct Colors	<b>5.390</b>	4.070	<b>5.750</b>	5.350	<b>6.310</b>	4.780
CVD Effectiveness Score	<b>0.928</b>	0.832	<b>0.922</b>	0.867	<b>0.938</b>	0.815

TABLE VI  
CVD-TYPE SPECIFIC PERFORMANCE: AUTOENCODER VS.  
ENCHROMA-CX1 GLASS EFFECT

Metric	Protanopia		Deuteranopia		Tritanopia	
	AE	Enchroma	AE	Enchroma	AE	Enchroma
Delta E	<b>6.959</b>	7.741	<b>5.308</b>	7.671	<b>9.753</b>	7.932
CCI	<b>0.025</b>	0.056	<b>0.011</b>	0.011	<b>0.047</b>	0.051
SSIM	<b>0.866</b>	0.908	<b>0.908</b>	0.916	<b>0.878</b>	0.907
Contrast	<b>0.998</b>	0.968	<b>0.995</b>	0.970	<b>0.995</b>	0.967
Color Variance	<b>215.059</b>	281.266	<b>218.611</b>	295.867	<b>216.809</b>	255.210
Distinct Colors	<b>5.320</b>	4.780	<b>5.820</b>	4.980	<b>6.160</b>	5.250
CVD Effectiveness Score	<b>0.852</b>	0.847	<b>0.862</b>	0.849	<b>0.885</b>	0.856

**Real-time Performance:** The autoencoder maintained inference speeds exceeding 280 FPS across all CVD types, making it suitable for real-time applications unlike traditional methods that often require specialized hardware. This computational efficiency, combined with superior color enhancement capabilities, positions our approach as a practical solution for real-world CVD assistance applications.

**CVD Effectiveness Score Analysis:** Based on the CVD Effectiveness Score, our autoencoder consistently outperformed both glass effect solutions, achieving a 10.9% improvement over Vino (0.929 vs. 0.838) and a 1.8% improvement over Enchroma-CX1 (0.866 vs. 0.851). This robust performance is evident in the type-specific results: for Protanopia, the autoencoder scored 11.4% higher than Vino and 0.6% higher than Enchroma; for Deuteranopia, it led by 6.4% and 1.5% respectively; and most notably for Tritanopia, it delivered a substantial 15.2% and 3.4% improvement, demonstrating its robust capability to enhance color perception across all major CVD types more effectively than traditional glass-based approaches.

## VIII. CONCLUSION AND FUTURE DIRECTIONS

This research presents a convolutional autoencoder method to improve images for people with color vision deficiency targeting protanopia, deuteranopia, and tritanopia. Using a rich and comprehensive set of images representing various landforms, the approach provided us with an algorithm-generated synthetic dataset through Daltonization that we could use for training our model to detect and alleviate color perception defects.

Results show that the model performed well in all our experiments, achieving high SSIM scores and low MS-SSIM loss, demonstrating excellent image reconstruction capabilities. The incorporation of skip connections proved crucial in preserving fine details and enhancing model learning. Most significantly,

our comprehensive comparative evaluation against traditional glass-based correction methods revealed the autoencoder's superior performance, improvement in color accuracy, color distinguishability and reduction in color confusion while maintaining real-time performances.

Our autoencoder demonstrated tangible improvements in color discrimination, indicating the feasibility of allowing colorblind individuals to perceive a broader color spectrum and enhanced visual perception. The comparison of original, daltonized, and reconstructed images confirmed the model's ability to effectively simulate and correct color-deficient vision. The demonstrated advantages over physical correction methods position our approach as a viable digital alternative that can be deployed across various platforms without the cost and accessibility limitations of specialized hardware.

In summary, vision studies for the color blind can directly benefit from our work, as this research advances the field of color-image enhancement with implications for photography, film, and digital content creation. The superior performance compared to traditional methods, combined with real-time processing capability, opens new possibilities for creating more inclusive visual experiences across diverse applications and platforms.

## ACKNOWLEDGMENT

We express our heartfelt gratitude to our Department of Electrical and Computer Engineering, North South University, Bangladesh for invaluable support, precise guidance and advice pertaining to the experiments, research and theoretical studies carried out during the course of the current project.

Furthermore, The authors also thank their loved ones for their countless sacrifices and continual support.

## REFERENCES

- [1] Anagnostopoulos, C., Tsekouras, G. E., Anagnostopoulos, I., & Kalloniatis, C. (2007). Intelligent modification for the daltonization process of digitized paintings. ResearchGate. [https://www.researchgate.net/publication/37683505\\_Intelligent\\_modification\\_for\\_the\\_daltonization\\_process\\_of\\_digitized\\_paintings](https://www.researchgate.net/publication/37683505_Intelligent_modification_for_the_daltonization_process_of_digitized_paintings).
- [2] Brettel, H., Viénot, F., & Mollon, J. D. (1997). Computerized simulation of color appearance for dichromats. *Journal of the Optical Society of America A*, 14, 2647–2655.
- [3] Capilla, P., Diez-Ajenjo, M. A., Luque, M. J., & Malo, J. (2004). Corresponding-pair procedure: a new approach to simulation of dichromatic color perception. *Journal of the Optical Society of America A*, 21, 176–186.
- [4] Capilla, P., Luque, M. J., & Diez-Ajenjo, M. A. (2004). Looking for the dichromatic version of a colour vision model. *Journal of Optics A: Pure and Applied Optics*, 6, 906–919.
- [5] Dietrich, J. (2024). daltonize: Simulate and correct images for dichromatic color blindness. GitHub. <https://github.com/joergdietrich/daltonize>
- [6] Hunt, D. M., Dulai, K. S., Bowmaker, J. K., & Mollon, J. D. (1995). The chemistry of John Dalton's color blindness. *Science*, 267(5200), 984–988. <https://doi.org/10.1126/science.7863342>.
- [7] Lee, J., & Santos, W. P. D. (2011). An adaptive fuzzy-based system to simulate, quantify, and compensate color blindness. *Integrated Computer-Aided Engineering*, 18(1), 29–40. <https://doi.org/10.3233/ica-2011-0356>.

- [8] Li, H., Zhang, L., Zhang, X., Zhang, M., Zhu, G., Shen, P., Li, P., Ben-namoun, M., & Shah, S. A. A. (2020). Color vision deficiency datasets & recoloring evaluation using GANs. *Multimedia Tools and Applications*, 79(37–38), 27583–27614. <https://doi.org/10.1007/s11042-020-09299-2>.
- [9] Nam, J., Ro, Y. M., Huh, Y., & Kim, M. (2005). Visual content adaptation according to user perception characteristics. *IEEE Transactions on Multimedia*, 7(3), 435–445.
- [10] National Eye Institute. (2024, April 15). Color blindness. National Eye Institute. <https://www.nei.nih.gov/learn-about-eye-health/eye-conditions-and-diseases/color-blindness>.
- [11] Salih, A., Elsherif, M., Ali, M., Vahdati, N., Yetisen, A., & Butt, H. (2020). Ophthalmic Wearable Devices for Color Blindness Management. *Advanced Materials Technologies*, 5(8), 1901134. <https://doi.org/10.1002/admt.201901134>.
- [12] Schmitz, J. (2016, September 14). Daltonization. ixora.io. <https://ixora.io/projects/colorblindness/daltonization/>.
- [13] Science Museum blog. (2019, September 6). Colour Blindness on the Move: A Brief Literary and Cultural History. <https://blog.sciencemuseum.org.uk/colour-blindness-on-the-move-a-brief-literary-and-cultural-history>.
- [14] Shen, X., Feng, J., & Zhang, X. (2020). A content-dependent Daltonization algorithm for colour vision deficiencies based on lightness and chroma information. *IET Image Processing*, 15(4), 983–996. <https://doi.org/10.1049/ijpr2.12079>.
- [15] Viénot, F., Brettel, H., Ott, L., Ben M'Barek, A., & Mollon, J. D. (1995). What do colour-blind people see? *Nature*, 376, 127–128.
- [16] Viénot, F., Brettel, H., & Mollon, J. D. (1999). Digital video colourmaps for checking the legibility of displays by dichromats. *Color Research and Application*, 24, 243–252. <http://tsi.enst.fr/~brettel/colourmaps.html>.
- [17] Viénot, F., & Brettel, H. (2001). Color display for dichromats. *Proceedings of SPIE*, Vol. 4300, 199–207.
- [18] Vischeck site: [www.vischeck.com](http://www.vischeck.com).